Published in final edited form as:
Arterioscler Thromb Vasc Biol. 2012 May ; 32(5): 1150–1157. doi:10.1161/ATVBAHA.111.243626.

Intravascular Optical Coherence Tomography Detection of Atherosclerosis and Inflammation in Murine Aorta

Satoko Tahara[*], **Toshifumi Morooka**[*], **Zhao Wang**, **Hiram G. Bezerra**, **Andrew M. Rollins**, **Daniel I. Simon**, and **Marco A. Costa**

Harrington-McLaughlin Heart and Vascular Institute, University Hospitals Case Medical Center (S.T., H.G.B., D.I.S., M.A.C.), Cardiovascular Research Institute, Division of Cardiovascular Medicine, Case Western Reserve University School of Medicine (T.M., H.G.B., D.I.S., M.A.C.), and Biophotonics Laboratory, Department of Biomedical Engineering (Z.W., A.M.R.), Case Western Reserve University, Cleveland, OH

Abstract

Objective—The goal of this study was to evaluate the feasibility of imaging the aorta of apolipoprotein E–deficient (ApoE$^{-/-}$) mice for the detection of atherosclerosis and macrophages using optical coherence tomography (OCT) compared with histology.

Methods and Results—Atherosclerosis was induced by high-fat diet in 7-week-old ApoE$^{-/-}$ mice for 10 (n=7) and 22 (n=7) weeks. Nine-week-old ApoE$^{-/-}$ mice (n=7) fed a standard chow diet were used as controls. OCT images of a 10-mm descending aorta in situ were performed in 4 mice for each, and plaque and macrophages were determined at 0.5-mm intervals. Automated detection and quantification of macrophages were performed independently using a customized algorithm. Coregistered histological cross-sections were stained with hematoxylin-eosin, Mac-3, and von Kossa. Three mice in each group had en face OCT imaging to detect macrophages, which were compared with lipid-positive area with Sudan IV. OCT images were successfully acquired in all mice. OCT and histology were able to discriminate macrophages and plaque among the 3 groups and showed excellent correlation for (1) visual detection of plaque (r=0.98) and macrophages (r=0.93), (2) automated detection and quantification of macrophages by OCT versus Mac-3-positive area (r=0.92), and (3) en face OCT detection of macrophages versus Sudan IV–positive area (r=0.92).

Conclusion—Murine intra-aortic OCT is feasible and shows excellent correlation with histology for detection of atherosclerotic plaque and macrophages.

Keywords

atherosclerosis; macrophages; optical coherence tomography

Correspondence to Marco A. Costa, MD, PhD, Harrington McLaughlin Heart and Vascular Institute, University Hospitals Case Medical Center, Case Western Reserve University, 11100 Euclid Ave, Cleveland, OH 44106. marco.costa@uhhospitals.org.
[*]S.T. and T.M. contributed equally to this work.

Disclosures

Dr Rollins has a modest financial interest from a licensing agreement with St. Jude/Lightlab Imaging. Dr Simon receives consulting fees and honoraria from Cordis/Johnson & Johnson and Medtronic Vascular. Dr Costa receives consulting fees and honoraria from Abbott Vascular, Medtronic, Scitech, Boston Scientific, Cordis/Johnson & Johnson, St. Jude/Lightlab Imaging, and Medtronic.

Preclinical animal models are indispensable in advancing our understanding of the pathophysiology of human disease and identifying new therapeutic targets. Murine models, in particular, enable rapid and precise genetic evaluation of specific human diseases and pathways. For example, apolipoprotein E deficiency ($ApoE^{-/-}$) is a well-established mouse model of atherogenesis that mimics key aspects of human atherosclerosis.[1–5] $ApoE^{-/-}$ mice develop atherosclerotic lesions containing lipid and inflammatory cells that are enhanced significantly by high-fat feeding.[1–6]

The evaluation of plaque and arterial wall inflammation in pre-clinical models requires harvesting the aorta for disease assessment using histological techniques. More recently, molecular imaging has enabled noninvasive imaging of atherosclerosis,[7] but poor spatial resolution remains a limitation.

Intravascular optical coherence tomography (OCT) is a novel catheter-based imaging modality using near-infrared light, which provides high-resolution (≈10 μm) in vivo imaging of human atherosclerosis.[8,9] We hypothesized that the small size (0.019 inches in diameter) of the clinically available OCT image wire (LightLab Imaging, Westford, MA) would enable high-resolution imaging of mouse aorta and direct visualization of atherosclerosis and arterial wall inflammation. Therefore, the aims of this study were (1) to investigate the feasibility of intravascular OCT to image murine aorta in situ, and (2) to validate OCT detection of plaque macrophages using both visual assessment and a novel, automated quantitative image algorithm compared with standard histology.

Methods

Animal Models

Male wild-type C57BL/6 and $ApoE^{-/-}$ mice of the same genetic background were purchased from the Jackson Laboratory (Bar Harbor, ME). All mice were maintained in animal facilities at Case Western Reserve University School of Medicine. Animal care and procedures were reviewed and approved by the institutional animal care and use committees and performed in accordance with the guidelines of the American Association for Accreditation of Laboratory Animal Care and the National Institutes of Health. Seven-week-old $ApoE^{-/-}$ mice consumed a high-fat diet (HFD) (Clinton/Cybulsky Rodent Diet D12108 with 1.25% cholesterol, Research Diets, New Brunswick, NJ) for 10 (n=7) and 22 (n=7) weeks. Nine-week-old $ApoE^{-/-}$ mice (n=7) fed a standard chow diet were used as controls. All OCT and histological analyses described below were performed by investigators blinded to mouse age and diet.

In Situ Mouse Intra-aortic OCT Imaging

Mice were sedated with ketamine and xylazine (0.2 mL/25 g body weight) to be euthanized before OCT imaging. Anterior thoracotomy and laparotomy were performed to allow visualization and positioning of the OCT catheter and to facilitate subsequent coregistration with histology. Saline flushes were administered via a 23-gauge catheter inserted into the apex of the left ventricle for in situ pressure perfusion at 100 mmHg during OCT image acquisition to minimize light absorption by red blood cells. The 0.019-inch OCT image wire

(ImageWire, LightLab Imaging, Westford, MA) was inserted into the left femoral artery up to the top of the aortic arch (Figure 1). A time domain OCT system (M2CV OCT Imaging System, LightLab Imaging, Westford, MA) equipped with a 1310-nm broadband light source was used for imaging. Before image acquisition, the abdominal aorta was held at the proximal bifurcation of the left renal artery and at the top of the left common iliac artery with 2 forceps to provide additional landmarks for coregistration of OCT and histology images. Images were acquired at a pullback speed of 1.5 mm/s. Immediately after the completion of aortic imaging, saline infusion was substituted with 4% paraformaldehyde under physiological pressure. The entire aorta was excised, immersed in buffered paraformaldehyde, and embedded in paraffin and subsequently processed for histology.

Histology

The descending thoracic aorta was used for histological examination, including routine light microscopy and immunohistochemistry (n=4 for each group). A 10-mm segment immediately proximal to the bifurcation of the left renal artery was sectioned (5 μm thickness) at 0.5-mm intervals. For immunohistochemistry, standard avidin-biotin procedures for mouse macrophage-specific marker Mac-3 (BD Pharmingen, San Diego, CA) were used. Immunostained sections were quantified as percentage positive area by image software (SigmaScan Pro version 5, Systat Software, Inc, San Jose, CA). Sudan IV staining was used to quantify atherosclerotic lipid-rich lesion area in an en face segment of the descending aorta (n=3 for each group). Quantification of Sudan IV stained lipid rich plaque area was done using computer-assisted imaging analysis (AxioVision Rel.4.5, Carl Zeiss, Thornwood, NY). Finally, von Kossa staining (American Mastertech Scientific Inc, Lodi, CA) was also performed to identify calcium hydroxyapatite.

Qualitative OCT Plaque Analysis

Acquired OCT images were analyzed offline at the Cardiovascular Imaging Core Laboratory, University Hospitals Case Medical Center (Cleveland, OH) by an independent expert blind to group assignments. The presence of plaque was determined at the same interval with histology sections of 0.5 mm along a 10-mm segment proximal to the left renal artery, and the correlation with histology was assessed. Plaque was defined as a thickened wall that disrupted a smooth, circular lumen contour (eg, protrusion).

Semiquantitative Macrophage Analysis

Macrophage semiquantification was performed on the same OCT cross-sections used for the qualitative plaque assessment. Previous reports[10,11] suggested that macrophages produce heterogeneous bright spots in the arterial wall on OCT images. Hence, we created an OCT macrophage grading system to semiquantify the bright spots based on axial and circumferential distribution, as follows: grade 0, no macrophage; grade 1, localized macrophage accumulation; grade 2, clustered accumulation <1 quadrant; grade 3, clustered accumulation ≥1 quadrant and <3 quadrants; and grade 4, clustered accumulation ≥3 (Figure 2 lower panel). Grading was performed in 2 manners: the entire aortic segment and specific segments with plaque (thickened wall). The possible ranges of the macrophage score were 0 to 80, which is a summation of 0 to 4 grades across all slices. Macrophage distribution on

histology was defined by Mac-3-positive staining and categorized in the same fashion as the OCT grading system described above.

Automated Quantitative Macrophage Analysis

Quantification of macrophages was based on a supervised classification method. The raw data (linear scale) of the OCT images was used for feature extraction. A training procedure was required before the actual application of the method. First, 12 OCT images from 3 mice involved in the Mac-3 staining experiments (2 on an HFD and 1 with normal diet, 4 images per mouse) with well-registered histology were selected by an expert as the training set. The imaging expert manually segmented macrophages in the training images based on the corresponding histology slides with custom-built software written in MATLAB (MathWorks, Inc). For every pixel within the vessel wall, the features, including intensity, SD and median intensity difference (MID), defined as the intensity difference of the central pixel and the median of its surrounding window, were recorded. For calculations of SD and MID, 4 different windows of sizes ranging from 82×82 to 136×136 μm^2 with an 18×18-μm^2 interval were used. This generated a total of 9 features for each pixel. Feature selection was performed using the "wrapper" model[12] with the J48 decision tree classifier (using the C4.5 algorithm[13–15]) and the Greedy forward search algorithm[12] by 10-fold cross-validation of the training pixels. Finally, only 6 features, including intensity, SD of 82×82- and 136×136-μm^2 windows, and MID of all windows except the 136×136-μm^2 window, were selected and used to train the final decision tree model. We then applied the decision tree to all OCT images (≈200/pullback and ≈1800 in total) of the 10-mm aorta segment of the remaining 9 mice involved in the Mac-3 staining protocol, which were used as the validation set. The classification was performed on the pixels within a presegmented vessel wall, which was generated first by lumen segmentation using a dynamic programming graph search algorithm discussed in detail elsewhere[16] and then by extracting the 100-μm-thick layer below the lumen surface. After the segmentation, the area of macrophages was quantified. The mean area per cross-section was correlated with the mean Mac-3 stained area as determined by histology. For the purpose of comparison, only the superficial 100 μm layer of the Mac-3-positive area was measured. Although we used age-matched mice under similar feeding conditions,[17] 1 validation mouse showed an extremely high accumulation of plaque with excessive positivity of Mac-3 staining at 29 weeks, and it was excluded from the final analysis.

En Face OCT Image Processing

The same algorithm was applied to the OCT images of the upper descending aorta from the 9 mice involved in the Sudan IV staining to create the en face images. The segmented macrophages were mapped to the surface of the lumen by maximum intensity projections. The luminal area of macrophages was quantified and correlated with the Sudan IV–positive area. Both areas were quantified relative to the total surface area of the lumen.

Mouse Survival Model

As a proof of concept for future longitudinal imaging studies, 2 additional (9-week and 17-week old ApoE$^{-/-}$) mice were imaged with OCT via the femoral artery, without thoracotomy or laparotomy, as no correlation with histology was necessary. Saline infusion

to minimize light absorption by red blood cells was performed via the other femoral artery, which was ligated at the end of the procedure. The goal was to acquire interpretable OCT images of the abdominal aorta and keep the animals alive after the imaging procedure.

Statistics

All analyses were conducted with SPSS Statistics 19 (IBM). Continuous variables were expressed as mean±SD, and categorical variables were expressed as frequencies. Probability values among the 3 groups were calculated using a Kruskal-Wallis test if the variable was continuous. For categorical variables, a χ test was used. Probability values <0.05 were considered significant. Correlation between OCT and histology was tested with Pearson correlation coefficients.

Results

OCT pullback images were successfully acquired in all mice. Figure 2 shows representative OCT images of the descending aorta of an ApoE$^{-/-}$ mouse after 22 weeks of high-fat feeding. A total of 240 cross-sectional OCT and histology paired images from 12 mice were assessed. Overall, 67% of OCT images showed atherosclerotic plaques identified as thickened tissues protruding into the aortic lumen, and 71% of OCT images contained focal areas of high backscattering strongly suggestive of macrophage accumulation. Importantly, because calcification had been reported to cause OCT bright spots, we performed von Kossa staining for calcium deposition. Histological staining for hydroxyapatite calcium was virtually absent even after high-fat feeding for 22 weeks, indicating that high backscatter regions represented macrophages rather than calcium deposition in this model. Figure 3 shows representative OCT cross-sectional images with corresponding hematoxylin and eosin, Mac-3, and von Kossa staining (a magnified image of von Kossa staining is presented in Figure I in the online-only Data Supplement).

Atherosclerotic Plaque Detection

Representative OCT images for plaque detection are shown as Figure II in the online-only Data Supplement. The thickness of the aorta wall without detectable plaque was 37.0±6.5 μm by OCT versus 30.3±3.1 μm by histology (P<0.001) in 9-week-old ApoE−/− mice fed with standard chow. Axial shrinkage rates on sections were not calculated; hence, correction of histology cross-sectional measurements was not performed. The numbers of OCT cross-sections showing atherosclerotic plaques were 2.5%, 73%, and 94% in the standard chow diet, 10-week HFD, and 22-week HFD groups, respectively (Table). Similarly, atherosclerotic plaques were detected by histological analysis in 0%, 72%, and 94% of mice in the standard chow diet, 10-week HFD, and 22-week HFD groups, respectively. OCT and histology showed excellent correlation for the determination of percentage of plaque-positive frames (r=0.98).

Semiquantitative Macrophage Assessment

We developed a semiquantitative grading system for macrophage accumulation by OCT. The possible ranges of the macrophage score were 0 to 80, which is summation of 0 to 4 grades across all slices analyzed. Aortic inflammation, as determined by OCT, was

significantly different between the standard chow diet (macrophage grade 6.25), 10-week HFD (24.3), and 22-week HFD (36.5) groups ($P<0.001$, Table and Figure 4A). When macrophage grading was applied exclusively to the plaque regions, the distribution shifted into lower grading categories (Figure 4B), with mean OCT macrophage grade of 0.25 in the standard chow diet, 22.0 in 10-week HFD, and 35.5 in 22-week HFD groups (Table). Macrophage (Mac-3-positive cells) accumulation was also graded histologically (Table and Figure 4C) and correlated with OCT (Figure 4D). There was a high correlation ($r=0.93$) between mean macrophage grade by OCT and mean macrophage grade by histology. In the standard chow diet group, OCT tended to overcall the detection of macrophages compared with histology. There were no macrophages detected in the standard chow diet group by histology.

Automated Quantitative Macrophage Analysis by OCT Versus Histology

We developed an automated macrophage detection algorithm for the quantification of macrophage accumulation by OCT. Macrophage area determined by the automated algorithm correlated highly with histological macrophage (Mac-3-positive cells) area (Figure 5A, $r=0.92$). Both OCT and histology were able to discriminate the degree of macrophage accumulation among the standard chow diet, 10-week HFD, and 22-week HFD groups (Table and Figure 5B); however, OCT overestimated macrophage area in all 3 groups compared with histology.

En Face OCT Assessment of Macrophage Accumulation Versus Sudan IV Staining

Atherosclerotic lesion area, as determined by en face staining for lipid accumulation of the opened and pinned aorta, is typically the primary end point in murine atherosclerotic studies. We therefore focused on examining the ability of OCT to quantitatively assess en face lesion area using the automated macrophage detection algorithm. The automated OCT method had strikingly similar spatial distribution as histological Sudan IV–positive area (Figure 5C and 5D). Excellent correlation ($r=0.92$, $P<0.001$) between automated OCT macrophage-rich area and Sudan IV–positive area was observed (Figure 5E).

Mouse Survival Model

Precise registration of OCT and histology required a nonsurvival experimental design. Our long-term goal is to develop an OCT imaging protocol that incorporates mouse survival, thereby establishing the foundation for repeat measurements over time. Two additional mice (1 ApoE−/− control and 1 $ApoE^{-/-}$ 10-week HFD) were imaged with OCT via the femoral artery without thoracotomy or laparotomy. OCT images were interpretable, and videos are provided (Videos I and II in the online-only Data Supplement) as proof of concept. Future technique refinements, standardization, and proper validation studies are required. Both mice survived >4 days before planned euthanasia.

Discussion

The present study is the first report of the feasibility of intra-aortic OCT high-resolution imaging for direct visualization and assessment of atherosclerosis in $ApoE^{-/-}$ mice. The data showed a high accuracy of OCT for plaque and macrophage detection compared with

histology, and the ability of OCT to discriminate plaque burden and macrophage accumulation among different treatment groups (standard chow diet, 10-week HFD, 22-week HFD). Additionally, the study validated a novel, automated algorithm for the quantitation of macrophage accumulation and atherosclerotic lesion area quantitative analysis.

The translation of preclinical discoveries to patients is likely to be accelerated when the same imaging modality is used across all species, from mice to large animals and humans. The success of molecular imaging using agents to target specific molecules or surface markers associated with vascular disease has been reported recently.[18–21] However, many experimental approaches are not approved for clinical use. The present study used a clinical imaging tool to investigate atherosclerotic lesion formation without the use of exogenous target or contrast agents.

OCT is a novel vascular imaging technology, which provides images with 10- to 20-μm axial resolution. The clinically available M3CV OCT Imaging System (LightLab Imaging, Westford, MA) acquires intravascular imaging using a 0.019-inch image wire, which is small enough to be applied in human coronary arteries and large conduit arteries of small animals. The ability of OCT to detect atherosclerosis and quantify macrophages in human coronaries with high accuracy is well documented in the literature.[10,11,22] Ex vivo imaging using a benchtop OCT system with shorter wavelength was used previously to detect plaque within the mouse aorta by placing the imaging source outside the vessel.[23] More recently, extravascular Fourier-domain OCT imaging of superficial small vessels has been used to test vascular function in murine models.[24] Although these extravascular imaging[23,24] studies support the ability of OCT to evaluate different aspects of vascular biology in preclinical models, the extravascular OCT approach is not applicable to humans because of limited tissue penetration of light and is not conducive to survival studies in animals afforded by intravascular approaches, as developed in the current study.

Our intravascular imaging approach using a clinically available OCT system enabled visualization of the entire vessel circumference and assessment of atherosclerotic plaques and macrophage accumulation within the entire vascular segment with high accuracy. The present study also describes a new, automated quantitative method to quantify macrophages in ApoE$^{-/-}$ mouse aorta, which showed excellent correlation (r=0.92) with histology. Automated quantification is desirable because it limits interobserver and intraobserver variabilities and can potentially reduce time and cost compared with conventional histology. Given the high speed of image acquisition, macrophage area on OCT images can be quantified in much smaller intervals as compared with histology (0.5 mm in this study), enabling a volumetric quantification of macrophages over the entire aorta tree. The previous method[10] to detect and quantify macrophage in human arteries was based on normalized standard deviation (NSD) within a region of interest (eg, fibrous cap) in the vessel wall. However, the use of NSD alone does not encompass all features of OCT signals generated by macrophages and may be prone to error; for instance, any region with dramatic changes in signals, such as tissue boundaries, has high NSD. Although the NSD method to detect macrophages was validated in ex vivo human arteries,[10] later modifications of the algorithm have yet to be validated.[11,25] The present study proposes a more comprehensive macrophage

detection method, capitalizing on the high-intensity images (bright spots) generated by macrophages in addition to a high NSD. A new metric, MID, is proposed to characterize the relationship of the central scatter (macrophage) with its surrounding scatters. Finally, the current method provides quantification of the absolute macrophage area, which represents an objective metric for preclinical and future clinical investigations. The translation of these methods into clinical studies will require further validation, but the ability to interrogate macrophage accumulation in more specific regions of interest, such as the fibrous cap, may further improve the accuracy of the method in human studies. It should be noted that the present methods can also be translated to different OCT systems but would require reselecting training images and rebuilding the decision trees.

The ApoE$^{-/-}$ mouse has been studied widely for atherosclerosis since its introduction.[5,6] The success of this animal model is mostly due to its availability, relatively easy breeding and colony maintenance, rapid development of atherosclerotic lesions with histopathologic progression, and ease of genetic manipulation with compound mutants.[20,21] The investigation of disease initiation, progression, and regression and the impact of therapies over time could be enhanced significantly by the use of repeatable, high-resolution imaging in longitudinal preclinical investigations, particularly if the same imaging method could be applied in humans. Although our preliminary survival model experiments are reassuring and established the first in vivo intravascular high-resolution aortic mice imaging, future studies are required to establish the value of this technique in longitudinal preclinical studies.

Limitations

We cannot rule out minor injury of the atherosclerotic vessel wall by the OCT catheter. Similarly, we cannot eliminate the influence of ligation of both femoral arteries on secondary systematic inflammatory response. Pressure perfusion fixation-induced aldehyde cross-linking of tissue proteins and plastic resin polymerization-induced shrinkage are inherent limitations of histology samples, which may have limited the exact coregistration of OCT and histology images.

The automated method detected a small degree of macrophage accumulation in ApoE$^{-/-}$ mice fed a standard chow diet despite the fact that there was no detectable Mac-3 staining. After carefully reviewing the corresponding OCT images, we confirmed the visualization of bright spots on OCT cross-sectional images. Importantly, OCT bright spots were not regions of calcification because calcium hydroxyapatite staining was negative. We hypothesize that speckles might also have contributed to these high-intensity signals. Speckles are caused by the interference of the backscattered OCT signal with random phases.[26] Because the OCT signal is based on nonspecific scattering of light in the tissue, once there is a high refractive index mismatch between adjacent scatters, a high-intensity signal is generated. However, it should be noted that this scenario, although possible, contributed to only a small portion of the detected bright spots because there was a high correlation between OCT and histology determined macrophage accumulation (Figure 5). Another possible explanation is that cholesterol crystals may produce high scattered OCT signals.[25] Furthermore, the incidence of false-positive macrophages may be further reduced by combining the information of plaque presence. Although detection of plaque was not included in the current algorithm, we

plan to include this step for human macrophage quantification in future clinical studies. Finally, the lack of plaque calcification (Figure III in the online-only Data Supplement) precludes generalization of the present study findings to models with more advanced atherosclerosis and calcified plaques.

The present study was limited to quantification of macrophage accumulation within 100 μm from the lumen surface. Macrophage assessment at deeper arterial wall layers, such as the adventitia, might not be feasible because of significant light attenuation. Similarly, it is not always possible to distinguish the surrounding connective tissue from the vessel wall (ie, external elastic membrane boundary) on OCT images, which precludes reproducible assessment of cross-sectional plaque or wall area. Finally, clinical catheter-based Fourier-domain OCT systems are not suitable for rodent models because of their large profile.

Supplementary Material

Refer to Web version on PubMed Central for supplementary material.

Acknowledgments

Sources of Funding

This work was supported in part by National Institutes of Health Grants HL85816 and HL57506 MERIT Award (to D.I.S.) and by the University Hospitals Harrington-McLaughlin Heart and Vascular Institute. LightLab Imaging (Westford, MA) provided the OCT console and catheters free of charge to conduct the experiments.

References

1. Plump AS, Smith JD, Hayek T, Aalto-Setala K, Walsh A, Verstuyft JG, Rubin EM, Breslow JL. Severe hypercholesterolemia and atherosclerosis in apolipoprotein E-deficient mice created by homologous recombination in embryonic stem cells. Cell. 1992; 71:343–353. [PubMed: 1423598]
2. Zhang SH, Reddick RL, Piedrahita JA, Maeda N. Spontaneous hyper-cholesterolemia and arterial lesions in mice lacking apolipoprotein E. Science. 1992; 258:468–471. [PubMed: 1411543]
3. Fazio S, Lee YL, Ji ZS, Rall SC Jr. Type III hyperlipoproteinemic phenotype in transgenic mice expressing dysfunctional apolipoprotein E. J Clin Invest. 1993; 92:1497–1503. [PubMed: 8376602]
4. Nakashima Y, Plump AS, Raines EW, Breslow JL, Ross R. ApoE deficient mice develop lesions of all phases of atherosclerosis throughout the arterial tree. Arterioscler Thromb. 1994; 14:133–140. [PubMed: 8274468]
5. Johnson JK, Carson K, Williams H, Karanam S, Newby A, Angelini G, George S, Jackson C. Plaque rupture after short periods of fat feeding in the apolipoprotein E-knockout mouse-Model characterization and effects of pravastatin treatment. Circulation. 2005; 111:1422–1430. [PubMed: 15781753]
6. Johnson JL, Jackson CL. Atherosclerotic plaque rupture in the apolipoprotein E knockout mouse. Atherosclerosis. 2001; 154:399–406. [PubMed: 11166772]
7. Jaffer FA, Vinegoni C, John MC, Aikawa E, Gold HK, Finn AV, Ntziachristos V, Libby P, Weissleder R. Real-time catheter molecular sensing of inflammation in proteolytically active atherosclerosis. Circulation. 2008; 118:1802–1809. [PubMed: 18852366]
8. Huang D, Swanson EA, Lin CP, Schuman JS, Stinson WG, Chang W, Hee MR, Flotte T, Gregory K, Paulifito CA. Optical coherence tomography. Science. 1991; 254:1178–1181. [PubMed: 1957169]
9. Tearney GJ, Brezinski ME, Bouma BE, Boppart SA, Pitris C, Southern JP, Fujimoto JG. In vivo endoscopic optical biopsy with optical coherence tomography. Science. 1997; 276:2037–2039. [PubMed: 9197265]

10. Tearney GJ, Yabushita H, Houser SL, Aretz HT, Jang IK, Schlendorf KH, Kauffman CR, Shishkov M, Halpern EF, Bouma BE. Quantification of macrophage content in atherosclerotic plaques by optical coherence tomography. Circulation. 2003; 107:113–119. [PubMed: 12515752]
11. MacNeill BD, Jang IK, Bouma BE, Iftimia N, Takano M, Yabushita H, Shishkov M, Kauffman CR, Houser SL, Aretz HT. Focal and multi-focal plaque macrophage distributions in patients with acute and stable presentations of coronary artery disease. J Am Coll Cardiol. 2004; 44:972–979. [PubMed: 15337206]
12. John, GH.; Kohavi, R.; Pfleger, K. Irrelevant features and the subset selection problem. Proceedings of the 11th International Conference on Machine Learning (ICML'94); San Francisco, CA: Morgan Kaufmann Publishers; 1994. p. 121-129.
13. Quinlan, JR. Programs for machine learning. Morgan Kaufmann; 1993. p. C4-C5.
14. Frank E, Hall M, Trigg L, Holmes G, Witten IH. Data mining in bioinformatics using Weka. Bioinformatics. 2004; 20:2479–2481. [PubMed: 15073010]
15. Dundar M, Fung G, Bogoni L, Macari M, Megibow A, Rao B. A methodology for training and validating a CAD system and potential pitfalls. International Congress Series. 2004; 1268:1010–1014.
16. Wang Z, Kyono H, Bezerra HG, Wilson D, Costa MA, Rollins A. Automatic segmentation of intravascular optical coherence tomography images for facilitating quantitative diagnosis of atherosclerosis. Proc SPIE. 2011:7889–7822.
17. Coleman R, Hayek T, Keidar S, Aviram M. A mouse model for human atherosclerosis: long-term histopathological study of lesion development in the aortic arch of apolipoprotein E-deficient (E0) mice. Acta Histochem. 2006; 108:415–424. [PubMed: 17007910]
18. McAteer MA, Akhtar AM, von Zur Muhlen C, Choudhury RP. An approach to molecular imaging of atherosclerosis, thrombosis, and vascular inflammation using microparticles of iron oxide. Atherosclerosis. 2010; 209:18–27. [PubMed: 19883911]
19. Graebe M, Pedersen SF, Højgaard L, Kjaer A, Sillesen H. 18FDG PET and ultrasound echolucency in carotid artery plaques. J Am Coll Cardiol Cardiovasc Imaging. 2010; 3:289–295.
20. Elmaleh DR, Fischman AJ, Tawakol A, Zhu A, Shoup TM, Hoffmann U, Brownell AL, Zamecnik PC. Detection of inflamed atherosclerotic lesions with diadenosine-5′,5″-P1, P4-tetraphosphate (Ap4A) and positron-emission tomography. Proc Natl Acad Sci U|S|A. 2006; 103:15992–15996. [PubMed: 17038498]
21. Tavakoli S, Razavian M, Zhang J, Nie L, Marfatia R, Dobrucki LW, Sinusas AJ, Robinson S, Edwards DS, Sadeghi MM. Matrix metalloproteinase activation predicts amelioration of remodeling after dietary modification in injured arteries. Arterioscler Thromb Vasc Biol. 2011; 31:102–109. [PubMed: 20947820]
22. Kume T, Akasaka T, Kawamoto T, Watanabe N, Toyota E, Neishi Y, Sukmawan R, Sadahira Y, Yoshida K. Assessment of coronary arterial plaque by optical coherence tomography. Am J Cardiol. 2006; 97:1172–1175. [PubMed: 16616021]
23. Cilingiroglu M, Oh JH, Sugunan B, Kemp NJ, Kim J, Lee S, Zaatari HN, Escobedo D, Thomsen S, Milner TE, Feldman MD. Detection of vulnerable plaque in a murine model of atherosclerosis with optical coherence tomography. Catheter Cardiovasc Interv. 2006; 67:915–923. [PubMed: 16602128]
24. Muller G, Meissner S, Walther J, Cuevas M, Koch E, Morawietz H. Analysis of murine vascular function in vivo by optical coherence tomography in response to high-fat diet. Horm Metab Res. 2009; 41:537–541. [PubMed: 19283654]
25. Stamper D, Weissman NJ, Brezinski M. Plaque characterization with optical coherence tomography. J Am Coll Cardiol. 2006; 47:69–79.
26. Schmitt JM, Xiang SG, Yung KM. Speckle in optical coherence tomography. J Biomed Optics. 1999; 4:95–105.

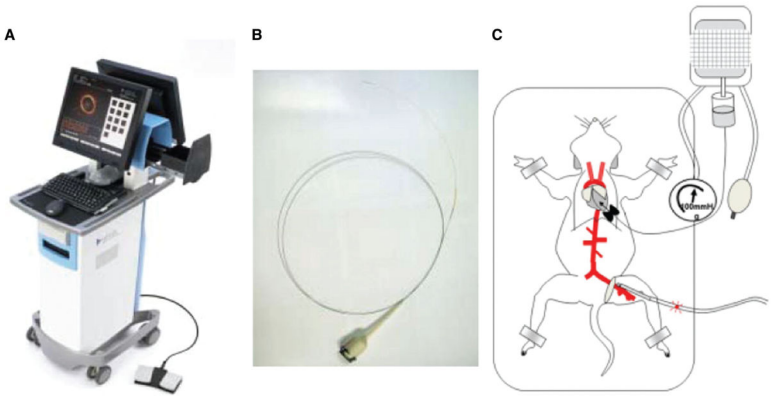

Figure 1.

Intra-aortic optical coherence tomography in a mouse apolipoprotein $E^{-/-}$ model. **A**, Optical coherence tomography (OCT) system console (M2CV OCT Imaging System, LightLab Imaging). **B**, OCT image wire. **C**, An illustration of experimental preparation of mouse intraaortic optical coherence tomography.

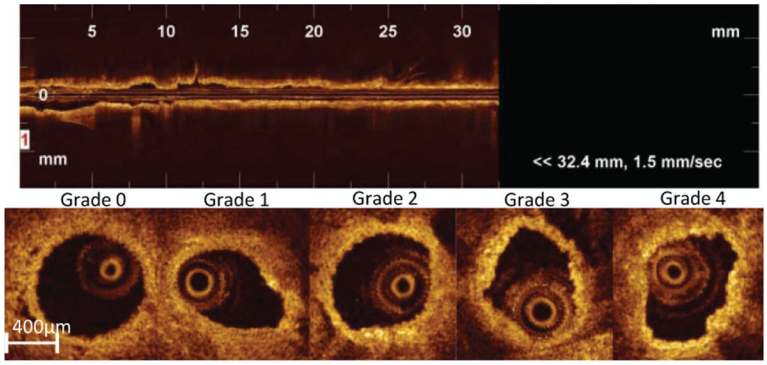

Figure 2.

Semiquantitative macrophage accumulation grading by intra-aortic optical coherence tomography (OCT). **Top panel** shows representative longitudinal OCT image of the entire mouse aorta. **Bottom panel** shows representative cross-sectional OCT images with the following grades: grade 0, no macrophage; grade 1, localized accumulation; grade 2, clustered accumulation in less than 1 quadrant; grade 3, clustered accumulation ≥1 quadrant and <3 quadrants; and grade 4, clustered accumulation ≥3 quadrants.

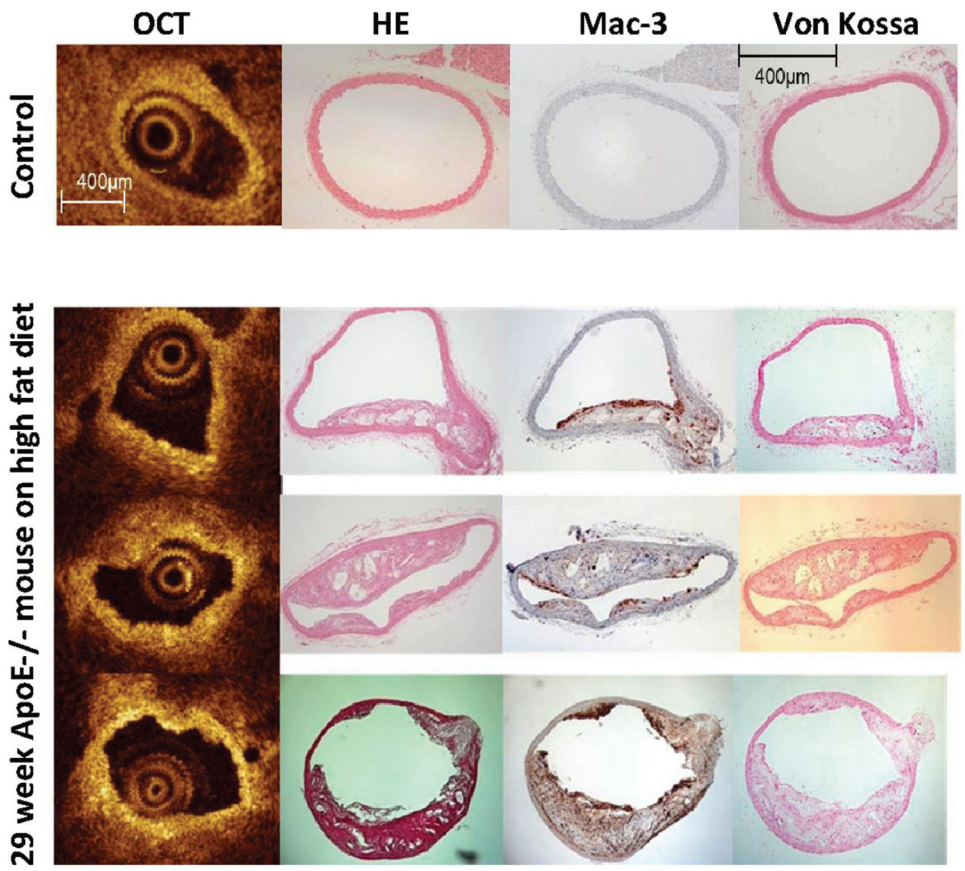

Figure 3.

Macrophage accumulation detected by intra-aortic optical coherence tomography (OCT) and immunohistochemistry in apolipoprotein E (ApoE)$^{-/-}$ mice. Shown are representative intra-aortic OCT cross-sectional images and corresponding hematoxylin and eosin staining (HE), Mac-3 staining, and von Kossa staining from a 9-week ApoE$^{-/-}$ mouse on standard chow diet (control, **top row**) and a 29-week ApoE$^{-/-}$ mouse on high-fat diet (**bottom 3 rows**) are shown. Accumulation of macrophages is shown as bright back-scattered reflections on OCT images. Note the smooth, circular contour of the OCT image (**top left panel**), corresponding to normal wall morphology by histology.

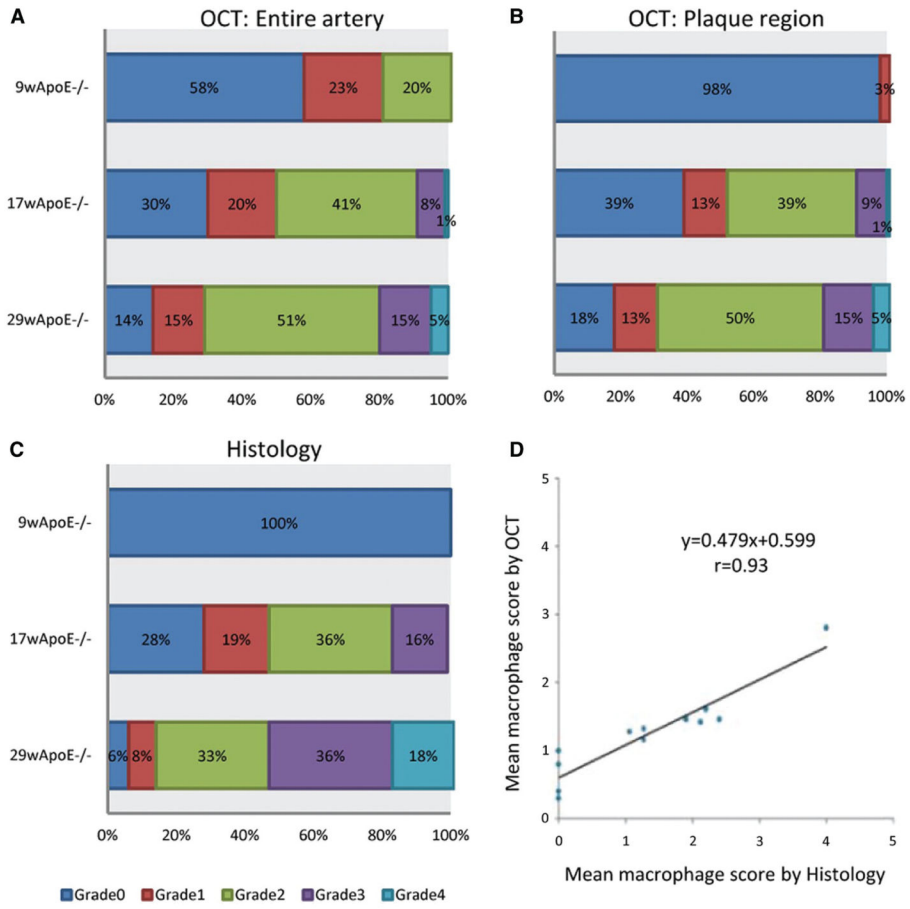

Figure 4.

Semiquantitative assessment of arterial wall macrophage accumulation. Distribution of optical coherence tomography (OCT) grades for macrophage accumulation in the entire arterial segment (**A**) is shown for each apolipoprotein E $(ApoE)^{-/-}$ diet group. Distribution of OCT and histology (Mac-3-positive area) grades of macrophage accumulation restricted to plaque regions is shown in **B** and **C**, respectively. **D**, Correlation between OCT- and histology-based macrophage accumulation grades.

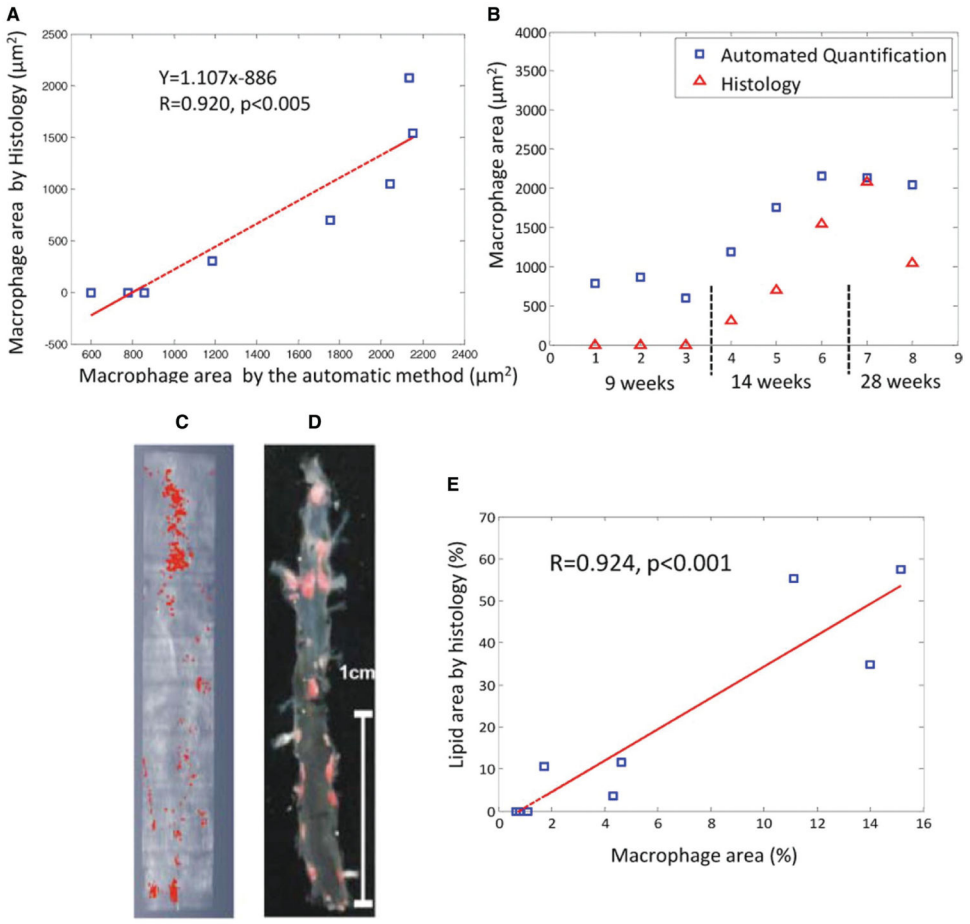

Figure 5.

Correlation between automated macrophage area quantification by optical coherence tomography and immunohistochemistry (Mac-3-positive area) in apolipoprotein E (ApoE)$^{-/-}$ mice for all ApoE$^{-/-}$ mice (**A**) and mice stratified by age/diet group (**B**). Macrophage area is represented as the mean area/cross-section. Shown are representative images of en face macrophage area (red) determined by the automatic optical coherence tomography (OCT) algorithm (**C**) vs Sudan IV staining for lipid accumulation (red) (**D**) of matched opened and pinned mouse aortas. Correlation between the automatic OCT quantified macrophage area and Sudan IV–positive lipid area in 9 ApoE$^{-/-}$ mice is shown in **E**.

Table 1

Table OCT and Histology Differentiation of Plaque and Inflammation in Different ApoE$^{-/-}$ Mouse Age Groups

	Control	17 w ApoE $^{-/-}$	29 w ApoE $^{-/-}$	*P*
Plaque				
OCT	2.5%	73%	94%	<0.001
Histology	0.0%	72%	94%	<0.001
Macrophage grade				
OCT (whole vessel)	6.25	24.3	36.5	<0.001
OCT (plaque only)	0.25	22.0	35.5	<0.001
Histology	0.0	26.5	43.3	<0.001
Macrophage area				
OCT	0.76 ± 0.11 μm^2	1.74 ± 0.41 μm^2	2.13 ± 0.05 μm^2	<0.001
Histology	0.00 ± 0.00 μm^2	0.85 ± 0.52 μm^2	1.56 ± 0.51 μm^2	<0.001

ApoE indicates apolipoprotein E; OCT, optical coherence tomography.